
TIME SERIES GENERATION WITH MASKED AUTOENCODER

Mengyue Zha

School of Mathematics

The Hong Kong University of Science and Technology

mzha@ust.hk

SiuTim Wong

School of Engineering

The Hong Kong University of Science and Technology

stwongak@ust.hk

Mengqi Liu

School of Statistics

Beijing Normal University

mqliu@bnu.edu.cn

Tong Zhang

School of Mathematics

The Hong Kong University of Science and Technology

tongzhang@ust.hk

Kani Chen

School of Mathematics

The Hong Kong University of Science and Technology

makchen@ust.hk

February 25, 2022

ABSTRACT

This paper shows that masked autoencoder with interpolator (InterpoMAE) is a scalable self-supervised generative model for time series. InterpoMAE masks random patches of the input time series and recover the missing patches in latent space. The core design is that no mask token is used. InterpoMAE disentangles missing patch recovery from the decoder. An interpolator directly recovers the missing patches without mask tokens. This design helps InterpoMAE to consistently and significantly outperforms state-of-the-art (SoTA) benchmarks in time series generation. Our approach also shows promising scaling behaviour in various downstream tasks such as time series classification, prediction and imputation. As the only self-supervised generative model for time series, InterpoMAE is the first in literature that allows explicit management on the synthetic data. Time series generation may follow the trajectory of self-supervised learning now.

1 Introduction

Time series models have witnessed a rapid growth of model capability and capacity since embracing deep learning. Latest models (eg. [1], [2]) tend to hundreds of millions of trainable parameters. The explosion of architectures is conditioned upon sufficient supply of high quality data. Many domains, however, fail to offer adequate qualified data. Most medical data contains sensitive personal information and cannot be directly shared. Financial data for events like recessions or flash crashes in the market is so scarce that studying the underlying mechanisms is nearly impossible [3]. Class imbalance and missing values also cause issues in time series problems [4]. The appetite for data has now been the bottlenecks of time series models based on deep learning.

A natural solution is generating synthetic data. We define synthetic data as any data that respects the temporal dynamics of original data and can be utilised as a substitute for the original data in real applications. We denote any model that produces synthetic data as the generative model. A basic requirement for the generative model is being able to produce adequate samples. One promising candidate is Generative Adversarial Networks (GAN) [5] which learns a mapping from random noises to the training data. By sampling from the random noises continuously, GAN generates an arbitrary number of samples. A line of work has focused on applying the unsupervised GAN framework to time series generation. The first (C-RNN-GAN) [6] takes Recurrent Neural Networks (RNN) as the generator and discriminator. Later, RCGAN [7] upgrades the RNN-based generator and discriminator with additional condition information. A multitude of studies

have applied GAN-variants to time series generation in various domains such as medicine (SC-GAN [8], NR-GAN [9]), finance (SigCWGAN [10]), sensor (SynSigGAN [11]) and decision making (DAT-CGGAN [12]). Nevertheless, none of these previous studies take into account the temporal nature of time series data. To better capture the temporal dependencies in time series data, TimeGAN [13] incorporates a supervised prediction task in the latent space of GAN. The embedding vectors of synthetic data are required to predict the embedding vectors of original data. To our best knowledge, TimeGAN is the only model that satisfies the second requirement for the generative model: generating diversified synthetic data while preserving temporal dynamics of the original data.

Despite the success of supervised training in TimeGAN, unsupervised paradigms still dominate time series generation. We ask: what differs in time series generation between unsupervised and supervised methods? We attempt to answer this question from the following perspectives:

1. The training complexity differs. Thanks to supervision from labelled training data, supervised generative models seldom suffer from problems running in the family of unsupervised generative models. Some typical problems are non-convergence, vanishing gradient and mode collapse [14]. These problems have been successfully addressed in natural language processing (NLP) and Computer Vision (CV) by self-supervised pre-training. The solutions, based on masked autoencoding in BERT [15] and MAE [16] are conceptually simple: they remove a portion of the data and learn to predict the removed content.
2. The manoeuvrability differs. Unsupervised generative models are born to be incompatible with extraneous supervision. GAN, for example, takes random noises as the seeds of generation and thus cannot be managed systematically. Supervised generative models allow us to take fine control on them. We may determine what kind of synthetic data to generate by changing the details of supervised learning directly (See Section 3.5 for more details).
3. The transferability differs. With the help of supervised training, we are able to generate synthetic data for various downstream tasks such as classification, prediction and imputation (See Section 3 for more details). Synthetic data generated by unsupervised models, however, is blind to the downstream tasks. Moreover, unsupervised generative models fail to impute missing values in time series for being lacking supervision from the ground truth.

The comparison provides us sufficient reasons to abandon the unsupervised paradigm. We propose a masked autoencoder with interpolator (InterpoMAE), a simple, effective and scalable supervised model for time series generation. Our InterpoMAE randomly masks some patches of the input time series and reconstructs the masked patches in the feature space. This design enables efficient and effective capture of temporal dynamics with bidirectional information. The model consists of three parts: an encoder, an interpolator and a decoder. The encoder only handles unmasked patches. Once the encoded latent representation of unmasked patches is ready, we interpolate it into latent representation for all patches (both masked and unmasked ones). Next, the decoder reconstructs the input from the interpolated latent representation. Unlike previous models with masking (eg. [15], [17], [16]), We do not use mask tokens. Instead, a fully connected layer learns the latent representation of masked patches by interpolation. This results in a large improvement in the performance. We also cut off popular stacked Transformer blocks in previous masking-based models (eg. [15], [17], [16]) and replace them by lightweight vanilla RNNs. The cutting off reduces the training time as well as the memory consumption, enabling us to easily scale our InterpoMAE to different downstream tasks. Under this design, our InterpoMAE infers holistic reconstruction even under an extreme high mask ratio (eg. 95%).

2 Approach

To learn temporal dynamics, Masked Autoencoder with Interpolator (InterpoMAE) recovers the original signal from its partial observations. The intuition behind the task is quite simple. A model that captures temporal patterns should be able to understand the context and predict on any blanks. Unlike prediction where only unknown sequences in the future are masked, generation allows for multiple masking strategies.

Masking. We denote the length of original time series as L and the number of features as k . InterpoMAE slices a single piece of discrete multivariate time series $x \in \mathbb{R}^{L \times k}$ into regular non-overlapping T patches $x_{1:T}$. Each of the T patches is an matrix $x_i \in \mathbb{R}^{l \times k}$, $i = 1, \dots, T$, living in the feature matrix space \mathcal{X} . We then sample a subset of N patches $x_{1:N}$ to reserve and remove the reInterpoMAEning ones. The patches to reserve are sampled from a uniform distribution without replacement. The length of each patch $l = \frac{L}{T}$ is determined by L , the length of the original time series and T , the number of patches. We assume that once a patch $x_i \in \mathbb{R}^{l \times k}$ is masked, all of the k features across l positions are invisible at the same time. Only the unmasked patches $x_{1:N}$ will be sent to the encoder.

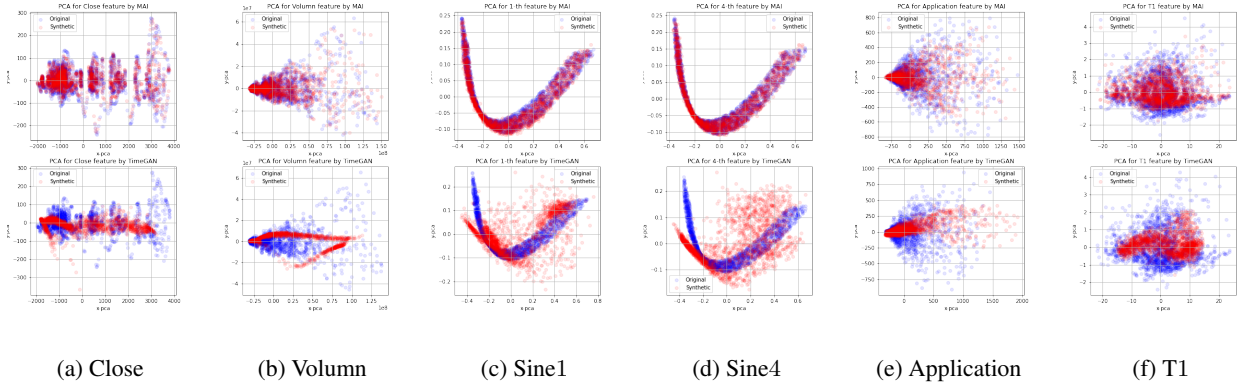


Figure 1: PCA visualisation on InterpoMAE (1st row) and current SoTA TimeGAN (2nd row) across six randomly selected features. Each column provides the visualisation of one feature. Visualisation on more features and benchmarks can be found in the Appendix.

Encoder. Our encoder only operates on visible, unmasked patches. The encoder maps visible patches in feature matrix space \mathcal{X} to their latent representations in latent matrix space \mathcal{H} . We denote the encoder as a function $E : \prod_{n=1}^N \mathcal{X} \rightarrow \prod_{n=1}^N \mathcal{H}$ from unmasked patches $x_{1:N}$ to their latent representations $h_{1:N}$.

$$h_{1:N} = E(x_{1:N}).$$

We implement E as stacked recurrent neural networks with a fully connected layer in the end. Just like previous work, our encoder E embeds the underlying temporal dynamics of original data into lower dimensions by a linear projection. However, our encoder only operates on visible patches and no mask tokens are used.

Interpolator. The interpolator restores the latent representations of masked positions. We denote the interpolator as a function $I : \prod_{n=1}^N \mathcal{H} \rightarrow \prod_{t=1}^T \mathcal{H}$ that fills in the missing latent representations from visible neighbouring patches $h_{1:N}$. The interpolator gives latent representations $\tilde{h}_{1:T}$ for all T patches as the outputs.

$$\tilde{h}_{1:T} = I(h_{1:N})$$

We implement I as stacked fully connected layers.

Decoder. The decoder $D : \prod_{t=1}^T \mathcal{H} \rightarrow \prod_{t=1}^T \mathcal{X}$ recovers latent representations $\tilde{h}_{1:T}$ to the synthetic data $\hat{x}_{1:T}$.

$$\hat{x}_{1:T} = D(\tilde{h}_{1:T})$$

We implement D as stacked recurrent networks with a fully connected layer in the end. In previous work, the role of decoder is two fold: (i) restoring information being masked. (ii) mapping the latent representations back to feature space. This design requires the introduction of mask tokens. Mask token is a learned special token that indicates the presence of missing patches. Previous works use the mask token as the mark for patches to be predicted by the decoder. Though mask token works well, most of these methods are for solving NLP problems where the latent representations for text data are usually highly discrete. In contrast, most time series data takes continuous values. We note that the predictions cluster in the restored patches after introducing mask tokens. To tell the decoder location information about the mask tokens, we need to add positional embeddings to the latent representations. This may further spoil the time series data.

The key insight in our work is that no mask token should be introduced. We disentangle missing patch recovery from latent representations decoding. In InterpoMAE, the interpolator specialises in (i) and the decoder is only responsible for (ii). Since the decoder no longer recovers missing patches, we avoid applying mask tokens and positional embeddings to the decoder.

Reconstruction target. Our InterpoMAE reconstructs the input by predicting the values for each masked patch. The last layer of the decoder is a linear projection that produces reconstructed time series $\hat{x}_{1:T}$. Our loss function computes

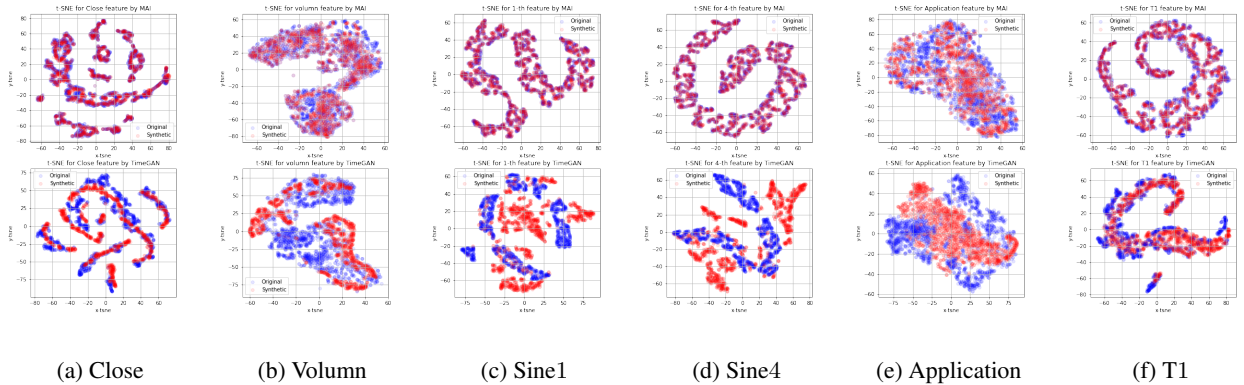


Figure 2: t-SNE visualisation on InterpoMAE (1st row) and current SoTA TimeGAN (2nd row) across six randomly selected features. Each column provides the visualisation of one feature. Visualisation on more features and benchmarks can be found in the Appendix.

the mean squared error (MSE) between the reconstructed and original time series in feature matrix space \mathcal{X} . We denote the loss of reconstruction as \mathcal{L}_{recon} . Unlike BERT [15] and MAE [16] where only loss on masked patches are computed, we take all patches into consideration (The index of patch t runs from 1 to T). (Requirement by continuity)

$$\mathcal{L}_{recon} = \mathbb{E}_{x_{1:T} \sim p} \left[\sum_{t=1}^T \|x_t - \hat{x}_t\|_2 \right],$$

where p stands for the unknown underlying distribution of the original time series.

3 Experiments

There are three desiderata for a time series generative model. (1) fidelity: the produced synthetic data should preserve the temporal dynamics of the original data. (2) practicality: the produced synthetic data should be able to substitute the original training data in real applications. (3) manoeuvrability: the generative model should endow users with explicit managements on the synthetic data, for example, the degree of fidelity and properties related to downstream tasks.

3.1 Visualisation

We first give intuitive evaluation on fidelity by visualisation. We apply t-SNE [18] and PCA [19] to show how closely the distribution of the synthetic data resembles the distribution of the original data.

Baseline: TimeGAN. We use TimeGAN as the backbone in visualisation. TimeGAN is the current state-of-the-art method for time-series data generation. It captures the temporal dynamics by an innovative combination of the unsupervised GAN and a supervised auto-regressive loss. Figure 1 and Figure 2 give an intuitive comparison between synthetic data generated by TimeGAN *vs.* synthetic data generated by InterpoMAE.

Visualisation In Figure 1 and Figure 2, InterpoMAE (1st row) are compared with the current SoTA TimeGAN (2nd row) across six features randomly selected from Sines, Stocks and Energy (The introduction to these three datasets are deferred until qualitative evaluation on fidelity). We project synthetic data (red) and original data (blue) into a two dimensional surface and see how well the red dots overlap with the blue ones. InterpoMAE shows strikingly better overlapping than TimeGAN in both PCA (Figure 1) and t-SNE (Figure 2) plots. Synthetic data (red) generated by InterpoMAE are in perfect sync with the original data (blue) while the manifolds of synthetic data (red) produced by TimeGAN are distinct from the manifolds of original data (blue). Visualisation on more features and benchmarks can be found in the Appendix.

3.2 Discrimination Scores

We then quantitatively evaluate the fidelity by discrimination scores. A post-hoc discriminator (a 2 layer LSTM [20]) is trained to distinguish between synthetic data and original data. We denote the discrimination scores as the post-hoc

classification errors given by the post-hoc discriminator. We evaluate our model on a variety of datasets with different statistics such as periodicity, discreteness, regularity, level of noise and degree of correlation.

Stock. Stock dataset records daily historical Google stock data from 2004 to 2019 with five features: high, low, opening, closing, adjusted closing prices and the volume. This continuous-value dataset is characterised by aperiodic as well as strong correlation between the features.

Sine. Sine data $\mathbf{x}(t)$ is generated through program simulation, and the generating function is $x_i(t) = \sin(2\pi ft + \phi)$ for each dimension $i \in \{1, 2, 3, 4, 5\}$, where frequency $f \sim U(0.03, 1)$ and phase $\phi \sim U(-\pi, \pi)$. This data is characterised by its continuity, periodicity, multivariate sequences and independent features.

Energy. Energy data is acquired from UCI Appliances Energy Prediction Data Set, consisting of numerous measured features of appliances energy use in a low energy building. This data has characteristics as high dimensional variables, continuity and noisy periodicity. Detailed statistics of each dataset can be found in the Appendix.

To more comprehensively demonstrate the fidelity of InterpoMAE, we compare the discrimination scores of InterpoMAE with two more unsupervised generative models, RCGAN and C-RNN-GAN.

RCGAN. RCGAN is a conditional GAN model with a focus on medical time-series data. RCGAN introduces additional information from associated labels as the condition and uses stacked LSTMs layers to process the condition recurrently.

C-RNN-GAN. C-RNN-GAN is a GAN model for continuous sequential data. It implement the generator by RNN but use bidirectional RNN for the discriminator. Specifically, Freezing is applied to both generator and discriminator to prevent one network being too strong and fooling the other entirely.

Table 1 summarizes the discrimination scores of all candidate models on the three datasets. We note that the self-supervised InterpoMAE produces the most indistinguishable synthetic data on all datasets in comparison with unsupervised benchmarks. InterpoMAE achieves 72%, 90%, 18% lower discrimination scores than the second runner-up in Stock, Sine and Energy respectively ($72\% \approx \frac{|0.071-0.256|}{0.256}$, $90\% \approx \frac{|0.019-0.184|}{0.184}$, $18\% \approx \frac{|0.410-0.499|}{0.499}$). The theoretical infimum of discrimination score is achieved when the synthetic data is replaced by original data. We mark the infimum as *Original* under discrimination scores in Table 1.

3.3 TSTR Experiments

We then show the practicality of InterpoMAE under the *Train on Synthetic Test on Real* (TSTR) framework [7]. In TSTR, a supervised model is trained by synthetic data but tested on the original data. We choose prediction and classification as two supervised tasks to see how well the synthetic data work under TSTR. Table 1 shows that the synthetic data generated by InterpoMAE consistently act as the best substitute for the original data across all datasets in both prediction and classification.

Prediction Scores Useful synthetic data is supposed to inherit the predictive characteristics from original data. Therefore, we expect the predictor trained by synthetic data from InterpoMAE makes the most accurate prediction when tested by original data. We take a simple two layer LSTM as the predictor and denote the mean absolute error of the predictor as the prediction score. Table 1 lists the prediction scores of all generative models on Sine, Stock and Energy. Smaller prediction scores are better. We note that InterpoMAE consistently achieves the best performance on TSTR prediction among all candidate models. Remarkably, prediction scores of InterpoMAE are 30%, 18%, 10% lower than the second runner-ups in Stock, Sine and Energy respectively ($30\% \approx \frac{|0.037-0.053|}{0.053}$, $18\% \approx \frac{|0.102-0.124|}{0.124}$, $10\% \approx \frac{|0.265-0.296|}{0.296}$). The theoretical infimum of TSTR prediction score is achieved when training the predictor by original data itself. We mark the infimum as *Original* under prediction scores in Table 1.

Classification Scores Similarly, we conduct *Train on Synthetic Test on Real* (TSTR) classification on various datasets. We take a simple three layer MLP [21] as the classifier. The classifier is trained on synthetic data but evaluated by original data. We denote the accuracy of the classifier as the classification score. Larger classification score means better accuracy. We selected three datasets from different doInterpoMAEens for TSTR classification.

Wafer. Wafer dataset relates to semiconductor microelectronics fabrication. Each data set in the wafer database contains the measurements recorded by one sensor during the processing of one wafer by one tool. The classification problem aims to distinguish between normal and abnormal.

IPD. IPD stands for Italy Power Demand. This dataset is derived from twelve monthly electrical power demand time series from Italy. The classification task is to distinguish days from October to March (inclusive) from April to September.

Strawberry. Strawberry data aims to classify food into two groups, Strawberry and non-Strawberry ,by food spectrographs. The data is obtained using Fourier transform infrared (FTIR) spectroscopy with attenuated total reflectance (ATR) sampling.

Detailed statistics of each dataset can be found in the Appendix.

Table 1: Scores on Discrimination, Prediction and Classification

METRIC	METHOD	STOCK	SINE	ENERGY
DISCRIMINATION SCORE	INTERPOMAE	.071 ± .020	.019 ± .010	.410 ± .107
	TIMEGAN	.256 ± .036	.184 ± .071	.499 ± .001
	RCGAN	.488 ± .001	.451 ± .033	.499 ± .000
	C-RNN-GAN	.500 ± .001	.500 ± .000	.499 ± .000
	ORIGINAL	.009 ± .005	.009 ± .004	.014 ± .003
PREDICTION SCORE	INTERPOMAE	.037 ± .000	.102 ± .000	.265 ± .001
	TIMEGAN	.053 ± .001	.124 ± .001	.302 ± .002
	RCGAN	.375 ± .013	.291 ± .000	.296 ± .004
	C-RNN-GAN	.086 ± .001	.749 ± .001	.498 ± .000
	ORIGINAL	.036 ± .001	.102 ± .001	.249 ± .000
METRIC	METHOD	WAFER	IPD	STRAWBERRY
CLASSIFICATION SCORE	INTERPOMAE	72.3 ± 0.92	83.9 ± 4.05	61.4 ± 2.01
	TIMEGAN	65.8 ± 1.01	54.3 ± 5.83	44.5 ± 1.71
	RCGAN	63.8 ± 1.15	57.0 ± 5.58	56.1 ± 1.20
	ORIGINAL	72.3 ± 1.59	81.3 ± 4.18	79.2 ± 1.89

3.4 Imputation Experiments

Table 2 shows that InterpoMAE achieves superb performance in time series imputation. Imputation requires the model to capture the complex distribution and the temporal dependencies in multivariate time series. Therefore, we expect InterpoMAE scales well on imputation. Due to the unsupervised nature, benchmarks in TSTR cannot be applied to imputation. We select a range of methods with different theoretic backups as the new benchmarks for imputation. Table 2 compares the imputation results of InterpoMAE and benchmarks. We note that InterpoMAE beats all benchmarks with markedly significant improvements. Comparing with the current state-of-the-art BRITS, InterpoMAE decrease 97% mean squared error and 86% mean absolute error on the Stock dataset ($97\% \approx \frac{|0.0007-0.0216|}{0.0216}$, $86\% \approx \frac{|0.0115-0.0802|}{0.0802}$). See Appendix for more details on imputation experiments.

Table 2: Imputation Results

METRIC	METHOD	STOCK	SINE	ENERGY
MEAN SQUARED ERROR (MSE)	MEAN	.0531 ± .0001	.0540 ± .0003	.0347 ± .0000
	MEDIAN	.0652 ± .0002	.0586 ± .0004	.0353 ± .0000
	SOFT	.0215 ± .0547	.0555 ± .1291	.0512 ± .0861
	KNN	.0214 ± .0547	.0496 ± .1311	.0434 ± .0844
	BRITS	.0216 ± .0039	.1608 ± .0060	.0092 ± .0054
	INTERPOMAE	.0007 ± .0001	.0069 ± .0059	.0088 ± .0009
MEAN ABSOLUTE ERROR (MAE)	MEAN	.1844 ± .0002	.1850 ± .0005	.1441 ± .0000
	MEDIAN	.1688 ± .0002	.1801 ± .0005	.1416 ± .0000
	SOFT	.0533 ± .1046	.1066 ± .1755	.1205 ± .1496
	KNN	.0500 ± .1061	.0716 ± .1863	.0920 ± .1433
	BRITS	.0802 ± .0156	.0757 ± .0245	.0420 ± .0241
	INTERPOMAE	.0115 ± .0032	.0494 ± .0214	.0365 ± .0073

Mean. Mean method replaces the missing entries with the mean of each column.

Median. Median method replaces the missing entries with the median of each column.

Soft. Soft [22] provides a regularised low-rank solution for large-scale matrix completion algorithms. It iteratively replaces the missing entries with the outcomes of soft-thresholded SVD.

KNN. KNN replaces the missing entries by weighted combination of k most related cases in the whole dataset.

BRITS. BRITS [23] is the current state-of-the-art method in time series imputation. It directly learns the missing entries in a bidirectional recurrent dynamical system.

3.5 Main Properties

Mask Ratio Figure 3 shows the influence of the mask ratio. We train InterpoMAE with a mask of different sizes (on the left) and different numbers of masks of size 1 (on the right). Table 3 shows the trend in practicality and fidelity when mask ratio grows. We evaluate practicality and fidelity by prediction scores and discrimination scores respectively. Fidelity fluctuates with growing mask ratio while there is no significant decrease in practicality when mask ratio goes to 12/24 and 7/24. To our surprise, InterpoMA generates the best synthetic data even when mask ratio goes to extremes (eg. 23/24). Full results in Appendix.

Table 3: Results of Different Number and Size of Masks on Stock Dataset

DATASET	SIZE	PRED	DISC	NUMBER	PRED	DISC
STOCK	1/24	.037 ± .000	.110 ± .116	1/24	.037 ± .000	.110 ± .116
	2/24	.037 ± .000	.055 ± .037	2/24	.037 ± .000	.128 ± .037
	3/24	.037 ± .000	.114 ± .106	3/24	.037 ± .000	.064 ± .106
	4/24	.040 ± .000	.145 ± .078	4/24	.038 ± .000	.077 ± .078
	6/24	.039 ± .000	.132 ± .100	5/24	.039 ± .000	.163 ± .100
	8/24	.039 ± .000	.102 ± .077	6/24	.041 ± .000	.127 ± .077
	12/24	.054 ± .001	.178 ± .019	7/24	.042 ± .000	.180 ± .077
ENERGY	1/24	.276 ± .010	.452 ± .019	1/24	.276 ± .006	.452 ± .022
	2/24	.277 ± .001	.440 ± .021	2/24	.275 ± .001	.415 ± .107
	3/24	.272 ± .001	.428 ± .014	3/24	.281 ± .004	.479 ± .019
	4/24	.310 ± .002	.439 ± .011	4/24	.278 ± .004	.485 ± .010
	6/24	.270 ± .002	.402 ± .119	5/24	.277 ± .005	.485 ± .005
	8/24	.278 ± .003	.376 ± .142	6/24	.289 ± .004	.487 ± .007
	12/24	.256 ± .000	.488 ± .014	7/24	.302 ± .009	.494 ± .002
SINE	1/24	.102 ± .000	.273 ± .181	1/24	.102 ± .006	.273 ± .181
	2/24	.103 ± .000	.402 ± .163	2/24	.103 ± .001	.364 ± .187
	3/24	.105 ± .001	.323 ± .176	3/24	.108 ± .002	.402 ± .172
	4/24	.101 ± .000	.113 ± .012	4/24	.124 ± .026	.408 ± .160
	6/24	.136 ± .065	.248 ± .084	5/24	.107 ± .000	.402 ± .073
	8/24	.162 ± .001	.376 ± .024	6/24	.110 ± .000	.322 ± .094
	12/24	.114 ± .004	.370 ± .026	7/24	.106 ± .000	.369 ± .049

Ablation Study Our first version of InterpoMAE includes some classic ideas in literature. We ablate these ideas to show that none of them contribute to the performance. [24] initialises model parameters by an autoencoder (Implemented in InterpoMAE by \mathcal{L}_{auto} below). TimeGAN [13] suggests taking a supervised embedding loss to better capture temporal dynamics (Implemented in InterpoMAE by L_{embed} below). BERT [15] proposes mask tokens and position embedding. All of these mechanisms, in fact, introduced mismatches between the pre-training and fine-tuning towards the target tasks in masked autoencoders. Therefore, our InterpoMAE only keeps \mathcal{L}_{recon} (See Section 2 for definition). No mask token or position embedding is used.

According to [24], we may pretrain the model to reconstruct $x_{1:T}$ without masking. We denote the objective function as *autoencoder loss*.

$$\mathcal{L}_{auto} = \mathbb{E}_{x_{1:T} \sim p} \left[\sum_{t=1}^T \|x_t - \hat{x}_t\|_2 \right]$$

Similar to TimeGAN [13], we may encourage the interpolator to restore latent codes for the masked patches. We denote the unmasked, visible patches as $x_{1:M}$ and $h_{1:M}$ to be their latent representations. The objective function is *embedding loss*.

$$\mathcal{L}_{embed} = \mathbb{E}_{x_{1:M} \sim p} \left[\sum_{m=1}^M \|h_m - \tilde{h}_m\|_2 \right].$$

$h_{1:M}$ are latent codes of masked patches produced by the encoder with all patches $x_{1:T}$ as the inputs. $\tilde{h}_{1:M}$ are the latent codes of masked patches restored by the interpolator with partial signal $x_{1:N}$.

Table 4 shows ablation study on \mathcal{L}_{auto} (A), \mathcal{L}_{embed} (E) and \mathcal{L}_{recon} (R). In mode AER, we train the InterpoMAE by three consecutive stages, using \mathcal{L}_{auto} , \mathcal{L}_{embed} and \mathcal{L}_{recon} one by one. We define mode ER, AR and R similarly. Details in Appendix.

Table 4: Ablation study on Stock.

MODE	PRED	DISC
AER	.038224 ± .000262	.100716 ± .068423
ER	.037853 ± .000210	.186477 ± .127078
AR	.037846 ± .000189	.085402 ± .069082
R	.037068 ± .000150	.071965 ± .020396

4 Conclusions

Simple algorithms that perform well lie in the core of deep learning. In this study, masked autoencoder with interpolator (InterpoMAE), a simple self-supervised method shows consistent and significant improvements over state-of-the-art benchmarks in time series generation. Our InterpoMAE demonstrates excellent practicality and fidelity. It also scales well on downstream tasks such as prediction, classification and imputation. The key insight in our work is that no mask token should be introduced. To avoid mask token, we disentangle missing patch recovery from the decoder. An interpolator recovers the missing patch by just a simple fully connected layer. In the minimalist design, our InterpoMAE is markedly better than all benchmarks while being much simpler and faster. To our surprise, InterpoMAE infers complex, holistic reconstructions even with an extreme mask ratio near 95%. We hope this property will inspire future work. Time series generation may now embark on the trajectory of self-supervised learning.

References

- [1] Jiehui Xu, Jianmin Wang, Mingsheng Long, et al. Autoformer: Decomposition transformers with auto-correlation for long-term series forecasting. *Advances in Neural Information Processing Systems*, 34, 2021.
- [2] Boris N Oreshkin, Dmitri Carпов, Nicolas Chapados, and Yoshua Bengio. N-beats: Neural basis expansion analysis for interpretable time series forecasting. *arXiv preprint arXiv:1905.10437*, 2019.
- [3] Samuel A Assefa, Danial Dervovic, Mahmoud Mahfouz, Robert E Tillman, Prashant Reddy, and Manuela Veloso. Generating synthetic data in finance: opportunities, challenges and pitfalls. In *Proceedings of the First ACM International Conference on AI in Finance*, pages 1–8, 2020.
- [4] Chenguang Fang and Chen Wang. Time series data imputation: A survey on deep learning approaches. *arXiv preprint arXiv:2011.11347*, 2020.
- [5] Ian Goodfellow, Jean Pouget-Abadie, Mehdi Mirza, Bing Xu, David Warde-Farley, Sherjil Ozair, Aaron Courville, and Yoshua Bengio. Generative adversarial nets. *Advances in neural information processing systems*, 27, 2014.
- [6] Olof Mogren. C-rnn-gan: Continuous recurrent neural networks with adversarial training. *arXiv preprint arXiv:1611.09904*, 2016.
- [7] Cristóbal Esteban, Stephanie L Hyland, and Gunnar Rätsch. Real-valued (medical) time series generation with recurrent conditional gans. *arXiv preprint arXiv:1706.02633*, 2017.
- [8] Lu Wang, Wei Zhang, and Xiaofeng He. Continuous patient-centric sequence generation via sequentially coupled adversarial learning. In *International Conference on Database Systems for Advanced Applications*, pages 36–52. Springer, 2019.
- [9] Yuki Sumiya, Kazumasa Horie, Hiroaki Shiokawa, and Hiroyuki Kitagawa. Nr-gan: Noise reduction gan for mice electroencephalogram signals. In *Proceedings of the 2019 4th International Conference on Biomedical Imaging, Signal Processing, ICBSP '19*, page 94–101, New York, NY, USA, 2019. Association for Computing Machinery.

- [10] Hao Ni, Lukasz Szpruch, Magnus Wiese, Shujian Liao, and Baoren Xiao. Conditional sig-wasserstein gans for time series generation. *arXiv preprint arXiv:2006.05421*, 2020.
- [11] Debapriya Hazra and Yung-Cheol Byun. Synsiggan: Generative adversarial networks for synthetic biomedical signal generation. *Biology*, 9(12):441, 2020.
- [12] He Sun, Zhun Deng, Hui Chen, and David C Parkes. Decision-aware conditional gans for time series data. *arXiv preprint arXiv:2009.12682*, 2020.
- [13] Jinsung Yoon, Daniel Jarrett, and Mihaela Van der Schaar. Time-series generative adversarial networks. *Advances in Neural Information Processing Systems*, 32, 2019.
- [14] Maciej Wiatrak, Stefano V Albrecht, and Andrew Nystrom. Stabilizing generative adversarial networks: A survey. *arXiv preprint arXiv:1910.00927*, 2019.
- [15] Jacob Devlin, Ming-Wei Chang, Kenton Lee, and Kristina Toutanova. Bert: Pre-training of deep bidirectional transformers for language understanding. *arXiv preprint arXiv:1810.04805*, 2018.
- [16] Kaiming He, Xinlei Chen, Saining Xie, Yanghao Li, Piotr Dollár, and Ross Girshick. Masked autoencoders are scalable vision learners. *arXiv preprint arXiv:2111.06377*, 2021.
- [17] Hangbo Bao, Li Dong, and Furu Wei. Beit: Bert pre-training of image transformers, 2021.
- [18] Laurens Van der Maaten and Geoffrey Hinton. Visualizing data using t-sne. *Journal of machine learning research*, 9(11), 2008.
- [19] Svante Wold, Kim Esbensen, and Paul Geladi. Principal component analysis. *Chemometrics and intelligent laboratory systems*, 2(1-3):37–52, 1987.
- [20] Sepp Hochreiter and Jürgen Schmidhuber. Long short-term memory. *Neural computation*, 9(8):1735–1780, 1997.
- [21] Paul J Werbos. Applications of advances in nonlinear sensitivity analysis. In *System modeling and optimization*, pages 762–770. Springer, 1982.
- [22] Rahul Mazumder, Trevor Hastie, and Robert Tibshirani. Spectral regularization algorithms for learning large incomplete matrices. *The Journal of Machine Learning Research*, 11:2287–2322, 2010.
- [23] Wei Cao, Dong Wang, Jian Li, Hao Zhou, Lei Li, and Yitan Li. Brits: Bidirectional recurrent imputation for time series. *Advances in neural information processing systems*, 31, 2018.
- [24] Mafalda Falcao Ferreira, Rui Camacho, and Luis F Teixeira. Autoencoders as weight initialization of deep classification networks for cancer versus cancer studies. *arXiv preprint arXiv:2001.05253*, 2020.